We are IntechOpen, the world's leading publisher of Open Access books
Built by scientists, for scientists

6,900
Open access books available

185,000
International authors and editors

200M
Downloads

154
Countries delivered to

Our authors are among the

TOP 1%
most cited scientists

12.2%
Contributors from top 500 universities

CLARIVATE ANALYTICS
BOOK CITATION INDEX
INDEXED

WEB OF SCIENCE™

Selection of our books indexed in the Book Citation Index
in Web of Science™ Core Collection (BKCI)

Interested in publishing with us?
Contact book.department@intechopen.com

Numbers displayed above are based on latest data collected.
For more information visit www.intechopen.com

Tumor Microenvironment Heterogeneity: A Review of the Biology Masterpiece, Evaluation Systems, and Therapeutic Implications

Irene Tadeo, Tomás Álvaro, Samuel Navarro and
Rosa Noguera

Additional information is available at the end of the chapter

Abstract

A tumor can be considered as a highly heterogeneous functional tissue, connected and dependent on the microenvironment, which sends and receives signals to and from the tumor tissue itself. Tumor cells alter the mechanical properties of the microenvironment in order to create favorable conditions for their proliferation. Stromal cells and non-cellular elements of the extracellular matrix (ECM), including the host immune system, the fibrous scaffolding, the fundamental substance, and blood vascularization can determine tumoral cell morphologies, functions, aggressiveness, and response to treatment, as well as an accurate assessment of prognosis of the patients. Robust morphometric digital pathology techniques that are able to standardize measurements and analyse whole sets of immunohistochemical images are called for to identify, describe, and quantify the elements of the ECM. The computer-automated segmentation algorithms are therefore required to increase the knowledge on the tumor microenvironment heterogeneity and to provide new therapeutic targets.

Keywords: Extracellular matrix, digital pathology, tumor microenvironment, heterogeneity, reticulin fibers, vascularization

1. Introduction

Many processes relevant to cancer, such as differentiation, maturation, and the malignant potential of tumor cells have all been shown to be influenced by extracellular matrix (ECM) stiffness [1]. In the general context of cancer, within the tumor ECM, various support cells

(fibroblasts, Schwann cells), tumor-associated immune cells, and vascular (blood and lymph) endothelial cells are found, lying among a network of various reticulin, collagen, and elastic fibers merged within the interstitial fluids (glycosaminoglycans, proteoglycans, and glycoproteins) and gradients of several chemical species, which constantly interplay with cells and provide much of the structural support available to parenchymal cells in tissues, providing tensile strength and flexibility [2, 3].

Numerous studies have demonstrated that the tumor ECM not only responds to and supports carcinogenesis, but actively contributes to tumor initiation, progression, and metastasis, and must not only be understood as a reactive neighboring, but also as an active contributor [4]. In fact, it has been published that chronic growth stimulation, ECM remodeling, alteration of cell mechanics, and disruption of tissue architecture are a non-genetic basis, influencing cancer progression [5–7]. Given the complexity both within and outside the cancer cell, and the interactions between cancer cells and the surrounding stroma, it is not surprising that a single perturbation within a tumor can create a cascade of changes in multiple pathways and networks, some of which may have lethal repercussions [8].

Tumor malignancy is driven, among other factors, by the remodeling of contiguous stromal tissue to foster growth, metastasis, and therapy resistance. Tumor cells alter the mechanical properties of the microenvironment to create favorable conditions for their proliferation and/or dissemination [9]. They promote stiffening of their environment, which feeds back to increase malignant behaviors such as loss of tissue architecture and invasion [10]. Matrix remodeling by tumor-associated stromal cells entails the assembly of a highly dense ECM, whose physicochemical attributes enhance malignancy through morphogenic deregulation, tumor cell proliferation, vascular recruitment, and stromal cell differentiation [11–13]. Both tumor and stromal cells produce and assemble a matrix of collagens, proteoglycans, and other molecules such as cytokines that hinder the transport of macromolecules and stimulate the otherwise quiescent host cells to initiate a variety of processes, including desmoplasia and angiogenesis [14, 15]. Mediated by increased deposition, unfolding, and crosslinking of fibrilar adhesion proteins, stiffening increases cell contractility which, in turn, can directly and indirectly modify gene expression via altering transcription factor activity and the release of matrix-bound pro-tumorigenic growth factors [16–19]. Similarly, changes in the microstructure, elasticity, distribution of pore sizes, chemical composition, and fiber arrangement due to ECM remodeling can control aspects of tumor cell phenotype such as adhesion, mechanics, and motility [20–24]. The speed of malignant cells *in vitro* is also affected by the geometry of the ECM. Human glioma cells move faster through narrow channels than through wide channels or in non-stretched 2D surfaces. This is thought to be triggered by an increase in the polarity of the traction forces between cell and ECM [25]. Recent publications describe that not only neoplastic ECM stiffness, but also the firmness of tumor cells play a significant role in tumor progression. Steadiness of tumor cells, especially the metastatic cells, is lower than that of the normal cells of the same sample, and is currently caused by the loss of actin filaments and/or microtubules, and the subsequent lower density of the scaffold [26, 27].

The study of ECM elements composing the architectural scaffolding and the blood vessels can be performed by means of automated or semi-automated quantification. This technique can

be used on histologic sections of all malignancies, providing important tumor characteristics such as the morphometric features and the spatial context of tumor and stromal cells at single-cell resolution. Differences in the ECM of different cancer subtypes can contribute to a more comprehensive understanding of the highly heterogeneous tumor microenvironment, and can provide abundant and novel targets for therapy.

2. Masterpiece of biology

2.1. Glycosaminoglycans

Since glycosaminoglycans (GAGs) have been recognized as essential players in critical biological processes regulating cellular properties, owing to their particular biofiltering, scaffolding, and cell anchoring properties, they have been related to diverse malignancies and they are now understood as key elements involved in cancer cell biology and novel therapeutical agents [28, 29].

GAGs are long, non-branched polymers of several disaccharides (up to 200 repeated saccharides), consisting of one uronic acid (almost always glucuronic acid and sometimes iduronic acid) and one hexosamine (glucosamine or galactosamine), presenting variable degrees of sulfation, and constitute the main components of the fundamental substance of the ECM [2]. According to their chemical composition, GAGs can be divided in acid and sulfated: chondroitin sulfate (CS), dermatan sulfate (DS), and heparan sulfate or heparin (HS, Hep); acid and non-sulfated: hyaluronan (HA); and non-acid and sulfated: keratan sulfate (KS). GAGs can form proteoglycans by means of a linkage tetrasaccharide, linking GAGs to a central protein (core protein) through a serine residue and catalyzed by four specific enzymes. The formation of the linkage tetrasaccharide is key for GAG synthesis to start in *GAGosomes* [30–32]. Proteoglycans can be located at the cell surface (syndecan, glypican), in the intracellular compartment (serglycin), secreted to the extracellular medium (small leucine-rich proteoglycans, hyalectans), or within the basement membrane (agrin, collagen XVIII, perlecan) [33, 34].

Diagnostic methods have typically centered on the analysis of GAG structure and concentration. Hyaluronan has the capacity to bind large amounts of water to form viscous gels with special filtering properties and it is capable of forming polyvalent connections with other ECM proteins. This GAG, as well as the rest, has the capacity of modulating host-tumor interaction, lymphangiogenesis, angiogenesis, and multidrug resistance. It can therefore be used as a drug carrier [35]. Hyaluronan accumulates in the stroma of various human tumors and modulates intracellular signaling pathways, cell proliferation, motility, and invasive properties of malignant cells: high stromal hyaluronic acid content is associated with poor differentiation and aggressive clinical behavior in human adenocarcinomas. On the contrary, squamous cell carcinomas and malignant melanomas tend to have a reduced HA content [35]. When tumors produce hyaluronan, this fact is associated with invasion, host-tumor interactions, lymphangiogenesis/angiogenesis, epithelial-mesenchymal transition and with local and distant metastases in glioma, pancreatic adenocarcinoma, breast cancer and prostate cancer, respectively [35]. Other studies in prostate carcinoma have found a link between poor prognosis and under-sulfation or overexpression of chondroitin sulphate. Aggressive breast cancer shows an

increase of approximately 15% on GAG content with longer chains compared to non-lethal breast cancer tissue [36].

2.2. Fibrous component

The architectural role of the fibrous component of the ECM is clear and central for tissue homeostasis. In fact, scaffold architecture has been found to have a significant impact on cell growth [37].

The primary proteins present in the ECM are the collagens. They are secreted by connective tissue cells, as well as by a variety of other cell types. As a major component of skin and bone, they represent the most abundant proteins in mammals, constituting 25% of the total protein mass in these animals. A typical collagen molecule is extremely rich in proline and glycine, long, stiff, and presents a triple-stranded helical structure, in which three collagen polypeptide chains called α chain are wound around one another in a ropelike superhelix [38]. Reticulin fibers, or type III collagen, are fine fibers forming an extensive branching network in certain organs. Their distribution is rather restricted: they are usually found mainly in the basement of epithelial tissues, the surface of adipose cells, muscle cells and Schwann cells, outside the endothelium of the hepatic sinusoids, and in the fibrous reticulum of lymphoid tissues. These fibers have a diameter of less than 2 μm and support not only the physical structure of the cell, but also various biological functions, largely through their ability to bind multiple interacting partners such as other ECM proteins, growth factors, signal receptors, and adhesion molecules [3, 39]. Collagen type I fibers account for 90% of the body collagen and usually form thick bundles in bone, skin, tendons, ligaments, cornea, and internal organs. These collagen strands measure up to 100 μm thick and usually follow a wavy course without branching in normal tissues.

The architecture of the collagen scaffolds in tumors is severely altered [18, 40]. It has been found that an aligned fiber matrix enhances differentiation of human neural crest stem cells towards the Schwann cell lineage [41] and evidence has pointed to collagen crosslinking as a significant contributor to the changes in cellular mechanical microenvironment that accompanies tumor progression [42]. Reticulin fibers are considered to play an important role in the adherence of cells and constitute a skeletal framework suitable for individual cells and tissues [43]. They are known to increase in amount and disorganize with aging and stress in physiological conditions [44]. Desmoplasia (collagen type I and reticulin fibers accumulation) is associated with several malignancies. The deregulation and disorganization of the tumor stroma alter the composition, structure, and stiffness of the ECM, leading to the creation of niches within tissues and organs that offer a proper environment for tumors to successfully establish metastasis and activate therapy resistance programs [40, 45, 46]. In primary breast tumors, collagen type I density is associated with breast cancer metastasis, and may serve as an imaging biomarker of metastasis. The expression of COL11A1 gene continuously increases during ovarian cancer disease progression, with the highest expression in recurrent metastases. Knockdown of COL11A1 decreases in vitro cell migration and invasion and tumor progression in mice [47]. The tumor-stromal interface of breast primary tumors in 3D culture was studied with second harmonic generation, showing that randomly organized matrix

realigned the collagen fibers allowing individual cells to migrate out along radially aligned fibers [48].

Elastic fibers are generally twisted or straight strands of 0.2–1.5 µm which sometimes branch to form a coarse network in loose connective tissue or form flattened sheets in dense elastic tissues such as the aorta [39]. As basic structural elements, elastic fibers aberrations trigger severe pathologies such as Marfan's syndrome, emphysema, hypertension, actinic elastosis, and aortic aneurysms [49]. Nevertheless, little evidence has been reported about its role in neoplastic processes. It has been found that elastic fiber increase, together with a decrease in collagen fibers is associated with oral squamous cell carcinoma and lymph node metastasis [50]. Elastin-rich lung ECM is largely remodeled during tumor invasion. The degradation of elastin produces peptides displaying a wide range of biological activities and increase invasive capacities of lung cancer cells by post-transcriptional regulation of metalloproteinase-2 [51]. This mechanism has also been found to act in melanoma progression, another cancer associated with rich elastin microenvironment [52].

2.3. Vascular component

Depending on their size and composition, blood vessels can be divided in capillaries (5–15µm), post-capillaries/metarterioles (15–20µm), sinusoids (20–50µm), venules/ arterioles (50–200µm), and veins/ arteries (>200µm). In order to grow over the limit of oxygen and nutrients diffusion, tumors have developed different strategies to provide blood supply. These mechanisms are sprouting angiogenesis: the growth of new capillary vessels out of preexisting ones; intussusceptive angiogenesis: the division of preexisting vessels in two new vessels by the formation of transvascular tissue in the lumen of the vessels; recruitment of endothelial progenitor cells or angioblasts; vessel co-option: tumor cells can grow along existing vessels without evoking an angiogenic response; vasculogenic mimicry: tumor cells dedifferentiate to an endothelial phenotype and make tube-like structures, providing tumors with a secondary circulation system; mosaic vessels: both endothelial cells and tumor cells form the luminal surface of the vessels [53–55].

In many aspects, tumor vessels are different from normal vessels. They are dilated, tortuous, and poorly covered by pericytes [56, 57]. The fact that tumor growth is dependent on angiogenesis has given rise to anti-angiogenic therapies targeting different pro-angiogenic molecules [58]. The tumor microenvironment comprises numerous signaling molecules and pathways that influence the angiogenic response. Understanding how these components functionally interact as angiogenic stimuli or as repressors and how mechanisms of resistance arise is required for the identification of new therapeutic strategies [59].

In some malignancies, different studies have shown conflicting results, some indicating a prognostic value of angiogenesis and others rejecting such conclusions [60–64]. This may arise from the fact that tissue vascularization has been quantified following different methods [62, 63], all based on the detection of the differential staining of the vessels with more or less specific immunostaining (anti-factor VIII, von Willebrand factor, CD34, CD31, caveolin or CD105) on image sections [65], hot spots [60], whole sections [62], or in tissue microarrays sections [64],

thereby indicating the need for robust morphometric techniques which may standardize the measurement of angiogenesis.

2.4. Immune system

The immune system is composed of different lineages of immune cells with different functions that protect every organism against infection. Among its tasks, immunosurveillance impedes transformed cells to become neoplastic cells. Indeed, increasing literature support the hypothesis that cancer development is influenced by the host immune system [66]. In fact, specialized blood vessels, the high endothelial venules (HEV), allowing the extravasation of lymphocytes, are present in primary human solid cancers [67, 68]. Therefore, it has been postulated that analyzing the composition, distribution, and architecture of the immune infiltrate for each tumor type, will offer new prognostic or predictive biomarkers [68, 69].

Immune infiltrates are heterogeneous between tumor types, and are diverse from patient to patient. All immune cell types may be found in a tumor, including macrophages, dendritic cells (DC), mast cells, natural killer (NK) cells, naïve and memory lymphocytes, B cells, and T lymphocytes (which include various subsets of T cell: TH1, TH2, TH17, regulatory T cells (TREGS), T follicular helper cells (TFH), and cytotoxic T cells). The analysis of the location, density, and functional orientation of different immune cell populations (termed the immune contexture) in large collections of annotated human tumors has allowed the identification of components that are beneficial for patients and those that are deleterious [70–72]. The prognostic impact of immune cells such as B cells, NK cells, myeloid derived suppressor cells (MDSC), macrophages, and subset of T helper populations (TH2, TH17, TREG cells) may differ depending on the type of cancer, and on the cancer stage [72]. In contrast, cytotoxic T cells, TH1 cells, and memory T cells were strongly associated with good clinical outcome for all cancer types [66, 72]. Notably, two large studies have shown that tumor immune infiltrate patterns and subsets in colorectal cancer are significant prognostic biomarkers [73, 74]. A potential clinical translation of these observations is the establishment of an Immunoscore, based on the numeration of two lymphocyte populations (CD3/CD45RO, CD3/CD8 or CD8/CD45RO), both in the core and in the invasive margin of tumors, as a clinically useful prognostic marker [75]. This immunoscore sheds light into the prognostic role of the tumoral immune infiltrate, but still needs to be validated in colorectal cancer. Its utility in other malignancies should be tested as well.

3. Methods for the quantification of ECM elements above mentioned

The methods explained are based on the experience of the group in the study of the ECM in neuroblastic tumor samples.

3.1. Samples

The study of tissue microarrays (TMAs) have emerged as a tool for rapid analysis for diagnostic and prognostic studies because several markers can be tested in huge amounts of samples [76–

79]. The main advantage of TMAs consists in the standardization of the methods, given that all samples contained in a single TMA are subject to the same protocols. TMA are mainly used to validate biologic markers with potential diagnostic value, which can be used to develop screening programs or enhance a subclassification of a disease [80]. The steps to follow are summarized in **Figure 1**. Alternatively, whole slides for individual samples can be used.
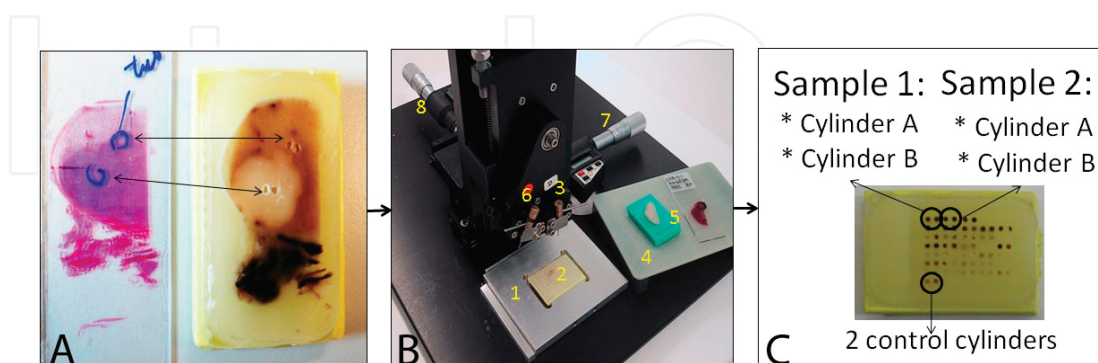
Figure 1. Steps followed to construct a TMA. **A)** Hematoxylin & eosin of a sample with two representative areas selected and their corresponding location in the paraffin block (already perforated). **B)** Beecher Instrument (Silver Springs, MD) and the different parts composing it (1 and 2: fixed plate and receptor block; 3: small needle to perforate the receptor block; 4 and 5: mobile plate with one donor block and its hematoxylin & eosin to be able to locate the representative regions selected by the pathologist; 6: big needle to extract cylinders from donor blocks; 7: fingerwheel to move in the X axis; 8: fingerwheel to move in the Y axis. **C)** TMA obtained where each sample is represented by 2 cylinders and 2 control cylinders are placed asymmetrically.

3.2. Stainings

Several serial sections of 3µm can be made and stained with histochemistry (HC) for GAGs, reticulin fibers and collagen type I fibers, and with immunohistochemistry (IHC) anti-CD31 for blood vessels.

Alcian blue pH 2.5 Stain Kit (Artisan™, Dako) stains acid GAGs (HS, CS, DS, and HA), sulfomucins and sialomucins in blue, the nucleus in red and the cytoplasm in pale pink (**Figure 2**).

Reticulin stains are silver stains based on the argyrophilic properties of reticulin fibers and a slightly modified Gomori can be used, which stains reticulin fibers in black (**Figure 3**). The first step in the staining procedure consists of oxidation of the hexose sugars in reticulin fibers to yield aldehydes. The second step is called sensitization in which a metallic compound such as ammonium sulfate is deposited around the reticulin fibers, followed by silver impregnation in which an ammonical or diamine silver solution is reduced by the exposed aldehyde groups to metallic silver. Further reduction of the diamine silver is achieved by transferring the sections to formaldehyde; this step is called revealing. The last step consists of toning by gold chloride in which the silver is replaced by metallic gold and the color of the reticulin fibers changes from brown to black. Masson's trichrome stain consists in the sequential staining with Harris hematoxylin which stains nuclei dark red, aniline blue which stains collagen and reticulin blue, and molybdic orange G which stains erythrocytes dark orange (**Figure 4**). Orcein

is a natural dye obtained from lichens which are found to stain elastic fibers dark brown (**Figure 5**).

CD31 is a single chain type 1 transmembrane protein with a molecular mass of approximately 135 kDa, belonging to the immunoglobulin superfamily. CD34 can also be applied to a subgroup, but this marker also stains cells other than endothelial. CD31 is expressed on endothelial cells of epithelial origin (all continuous endothelia, including those of arteries, arterioles, venules, veins, and capillaries, but it is not completely expressed on discontinuous endothelium in, for example, splenic red pulp). In addition, CD31 is expressed diffusely on the surfaces of megakaryocytes, platelets, myeloid cells, natural killer cells, and some subsets of T cells, as well as on B-cell precursors. Cells labeled by the antibody predominantly display membrane staining with weaker cytoplasmic staining (**Figure 6**).

Finally, IHC is used to detect diverse subpopulations of lymphocytes in tumoral tissues. For example, CD45 is a transmembrane glycoprotein expressed on most nucleated cells of hematopoetic origin, *i.e.,* all human leucocytes; CD20 reacts with an epitope located on the surface of B cells and appears early during B-cell maturation; CD3 is a pan-T cell marker for identification of T cells. It is well-suited for labeling reactive T cells in tissue with lymphoid infiltrates, and for classification of T-cell neoplasms; CD7 is expressed by the majority of peripheral blood T cells, NK cells, and all thymocytes. It is one of the earliest surface antigens on T and NK-cell lineages; CD4 is a transmembrane glycoprotein, expressed on normal thymocytes, T-helper cells, majority of mature peripheral T cells, and a subset of suppressor or cytotoxic T cells; CD8 is a 68 kDa transmembrane glycoprotein expressed as a heterodimer by a majority of thymocytes, and by class I major histocompatibility complex restricted, mature, suppressor/cytotoxic T cells; CD68 labels human monocytes and macrophages, but not myeloid cells; CD163 has been shown to mark cells of monocyte/macrophage lineage; CD11b is expressed on the surface of many leukocytes including monocytes, neutrophils, natural killer cells, granulocytes and macrophages, as well as on 8% of spleen cells and 44% of bone marrow cells; and CD11c is expressed prominently on the plasma membranes of monocytes, tissue macrophages, NK cells, and most dendritic cells (**Figure 7**).

3.3. Evaluation of the samples

3.3.1. Subjective assessment

The samples contained in TMAs or in whole slides can subjectively be analyzed by a pathologist to assess the amount of each ECM element as non-informative: artefact, scant material, lost cylinder; negative: no expression or <5% of stained area is detected; positive 1+: mild staining, 5–10% of the area; positive 2+: moderate staining, 10–50% of the area.; and positive 3+: strong staining, >50% of the area.

3.3.2. Automated quantification

The growing size and number of medical diagnostic images requires the use of computer-automated segmentation algorithms for the delineation of ECM structures of interest, which

play a vital role in the research of new biomedical-imaging markers [81]. This is critical to analyzing whole sets of HC and IHC images to identify, describe, and quantify tissue alterations of the ECM, and require digitation of the samples. Morphometric techniques based on computer-automated segmentation algorithms attempt to decrease human error, increase efficiency, assess large areas or huge amounts of tumor samples, create reproducible results, and help to standardize the measurements [81].

3.3.2.1. Digitization of the sections

The digitization of the samples is required to perform morphometric analysis. The method available in most laboratories is the capture of several images per sample with a photomicroscope. Sequential photos can be done at 20x or 40x magnifications with a photomicroscope and then carefully merged with Adobe Photoshop to reconstruct a single whole cylinder image (**Figure 2**). Following our experience, this method needs approximately two weeks to digitize 30 samples (2 cylinders per sample) for a single staining at 20x magnification, or approximately 6 to 7 weeks at 40x magnification.
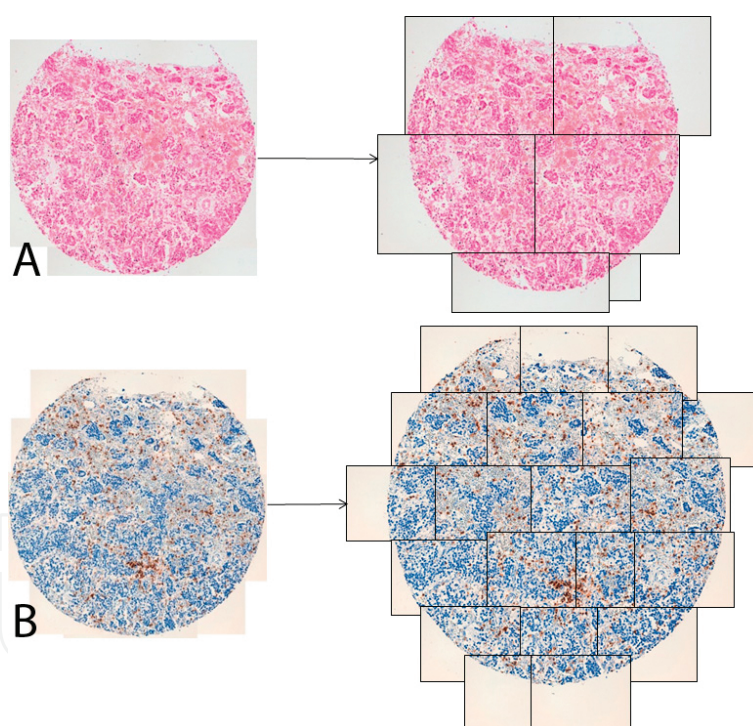

Figure 2. Process of hematoxylin & eosin and CD31 immunostaining TMA image capture. **A)** At 20x magnification, 6 individual images of the cylinder must be captured to reconstruct the whole cylinder image. **B)** The whole 1mm cylinder image at 40x magnification must be reconstructed from 20 individual images.

The use of a slide scanner is the only method that permits the digitization of a high number of cases for a reasonable time when developing a routine image biobank [82, 83] or a research project. Additionally, the use of slide scanners provides the possibility to standardize the image quality using preserved light conditions.

In order to enhance the standardization of the image capture conditions and therefore, the quality of the measurements and to save time, whole slide scanning is advised, as described next. Our group used the ScanScope XT scanner, Aperio technologies, but increasing alternatives such as Panoramic Midi from3D Histech and the Ventana iScann Coreo Au from Roche, among others can also be considered [82, 84]. ScanScope XT scanner is a brightfield scanner that digitizes whole sections at 20x or 40x magnification providing high resolution images in approximately 15 to 30 minutes per slide, depending on the magnification and the size of the tissue. 40x magnification was used, originating images with a resolution of 0.25 μm/pixel. Given to the enormous amount of pixels scanned, the images were compressed in JPEG2000 to 100–200 megabytes for the average size of a TMA, and saved to a proprietary TIFF format (SVS).

The sections were placed in a mobile plate one by one. An option for TMAs digitization provided by the scanner driver was used. This option recognizes the tissue cylinders and places several points per sample where the objective adjusts the focus to obtain clear and focused images. The mobile plate with the section moves in consecutive stripes, until it sweeps the whole section while the objective scans. Individual scanned stripes are originated and stitched together automatically to reconstruct the whole image, which can be visualized up to 40x magnifications with the Image Scope viewer software (Aperio technologies). The process is briefly shown in **Figure 3**.
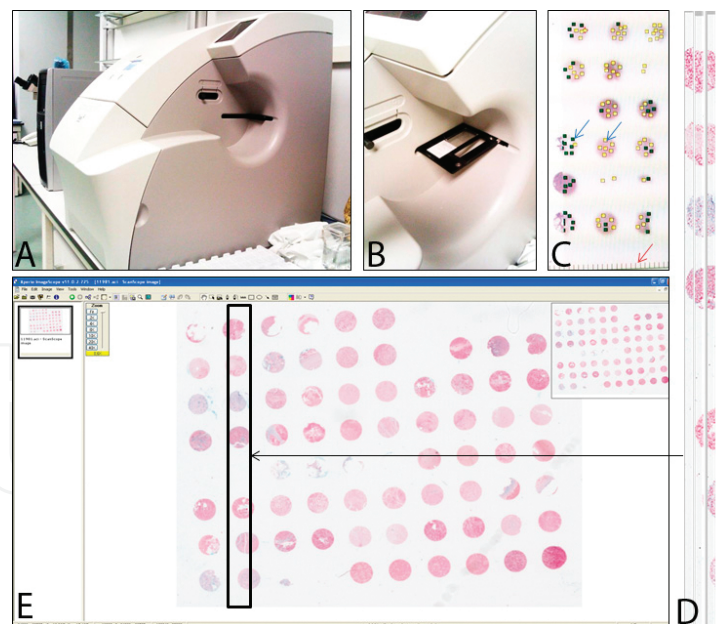
Figure 3. Digitization process. **A)** ScanScope XT, Aperio technologies. **B)** Mobile plate with one section on it. The plate is introduced in the scanner and placed under the objective to start the process. **C)** Preview of an area of the section. Blue arrows show the pre-set points where the scanner shall readjust the focus. Green points have already been properly focused and yellow points still have to be focused. The red arrow shows different marks corresponding to the different horizontal stripes which are going to be scanned individually and then stitched together. **D)** 4 single consecutive stripes are shown corresponding to the section in E. **E)** All the stripes are stitched to form a single image of the whole section. The image is opened in the free viewer ImageScope, Aperio technologies.

3.3.2.2. Design of automated image analysis algorithms

Depending on the staining to be measured and the availability of morphometric systems, different methods for image analysis can be used, all following a common workflow (**Figure 4**).
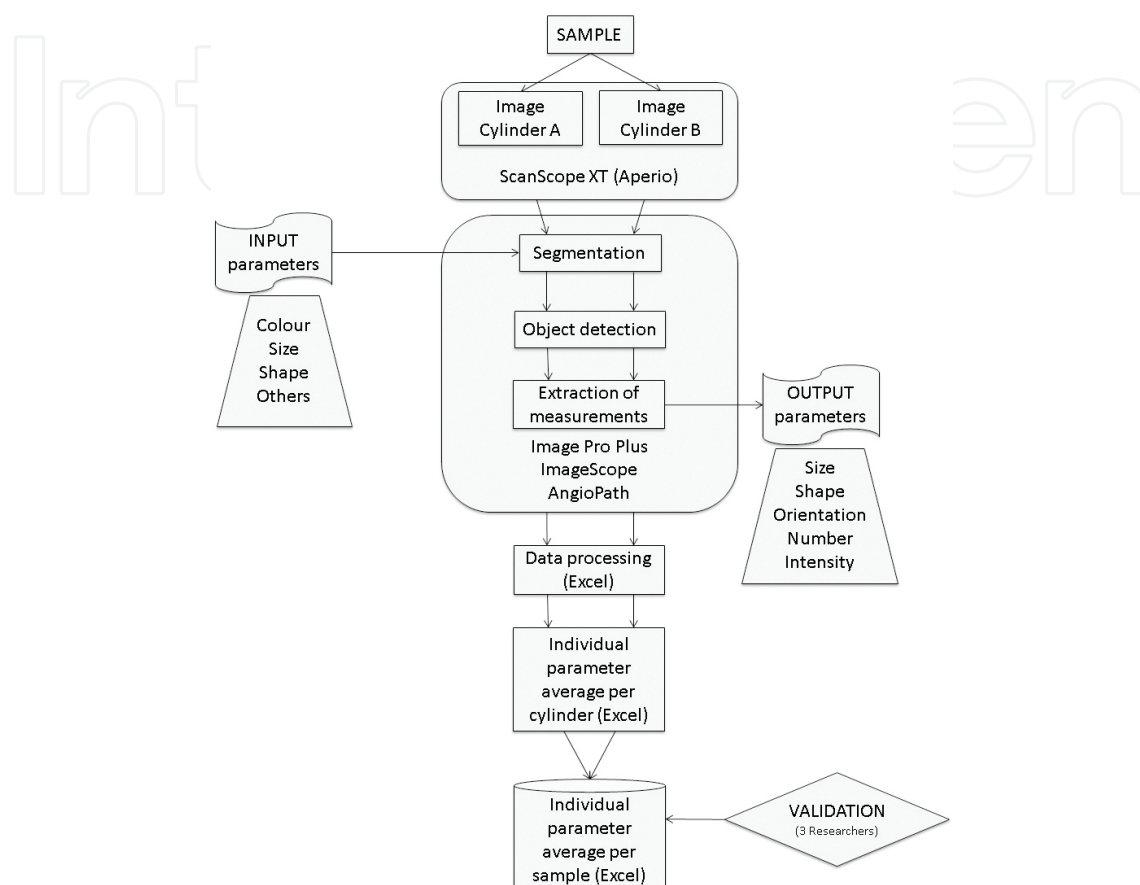

Figure 4. Flowchart showing the multi-resolution image analysis system for TMA with two cylinders per sample. Images belonging to different samples stained with different markers have been quantified by image analysis following a common process including segmentation (differential recognition of the staining) with specific input parameters for each marker and method and extraction of some given parameters. Adapted from Tadeo *et al.* [85].

OPTION 1: To use commercial software for image analysis with established protocols which the user can adapt to the marker specific color.

Example 1: Algorithm for the fundamental substance (GAGs). Each cylinder was analyzed individually with Aperio Positive Pixel Count Algorithm on Aperio ScanScope software by selecting each cylinder outline in the whole section image. This algorithm was used with the default parameters and counted the number of pixels belonging to a given staining intensity, being the intensity of each pixel the average between the values of red, green, and blue (RGB) intensities. It recognizes Alcian blue stained pixels which have average intensities over 221. Nuclear fast red stained pixels were detected with weak, middle, and strong intensities painted in yellow, orange, and brown following default parameters (**Figure 5**). The remaining customizable parameters were set by default.
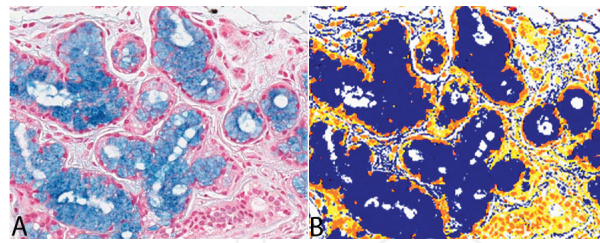
Figure 5. Segmentation obtained with the positive pixel count algorithm on a salivary gland. **A)** Original image. **B)** Mark-up image after segmentation. Alcian blue staining is marked in blue and nuclear fast red is marked in yellow, orange or maroon, depending on the intensity of staining.

Example 2: Algorithm for the immune system cells. Each cylinder was analyzed individually with the Nuclear Quant algorithm on Panoramic Viewer software (3D Histech) by selecting each cylinder outline in the whole section image. This algorithm was used with the default parameters and counted the number of cells presenting a given staining intensity. Stained cells were detected with weak, middle, and strong intensities painted in yellow, orange, and maroon (**Figure 6**).
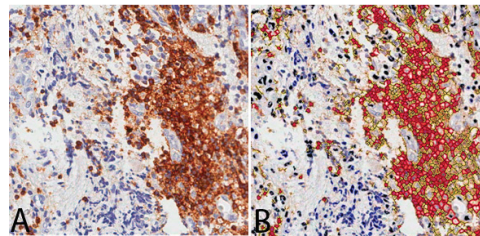

Figure 6. Segmentation of a neuroblastic tumor sample stained with IHC anti-CD45. **A)** Original image. **B)** Mark-up image after segmentation. Immune system cells are marked in yellow, orange or maroon, depending on the intensity of staining blue and hematoxylin is marked in blue.

> OPTION 2: To use commercial software for image analysis which allows the user to configure personal image analysis protocols or macros capable of recognizing and describing the specific color and shape of the element of interest.

Example: Algorithm for the reticulin fibers. The grading of fibrosis in general and namely of reticulin fibers is of main interest in bone marrow pathologies [86] and fibrous diseases of the liver [87]. For this reason, different methods for the quantification of reticular fibrosis have been developed, some of them consisting in automated morphometry [88–93]. However, these methods quantify the percentage of stained area and we considered that not only the amount of fibers, but also the morphometric features were relevant, given that these are usually subjectively assessed. Image Pro-Plus software (Media Cybernetics), which enables the design of specific algorithms, was used to analyze the fibrous component. An image of every cylinder was extracted in a separate JPEG-quality 80 image from the whole section scan. An algorithm capable of specifically detecting the reticulin fibers and measure their amount, size, and shape was customized. Image J is a free software providing similar options. An example of the segmentation process in a control tissue (kidney) is provided by **Figure 7**.
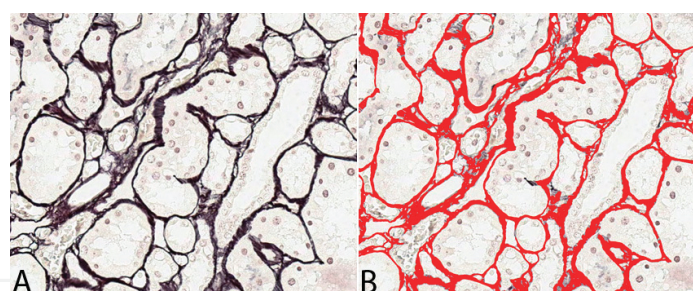
Figure 7. Segmentation process on a kidney tissue. **A)** Original image. **B)** Image after segmentation. The reticulin fibers recognized by the algorithm are marked-up in red.

OPTION 3: To design a personal application capable of solving commercial softwares lacks.

Example: Algorithm for the vascular component. A common feature of tumor vessels studies is that the researchers focus on microvessel density overlooking other parameters that might be significant, such as the size and shape of the microvessels [94]. Studies have revealed the importance of the size and shape of blood vessels in, for instance, laryngeal tumors [95]. The morphometric tool Angiopath closes blood vessels with discontinuous endothelial layer, recognizes all blood vessels and classifies them in six categories corresponding to different types of vessels, differentiated by their largest diameter or length. Density (density and occupied area), size (area, width, length, and perimeter), and shape (perimeter-ratio, shape index, branching, aspect, roundness, and deformity) parameters are extracted [96, 97]. An example of the segmentation process is provided in **Figure 8**.
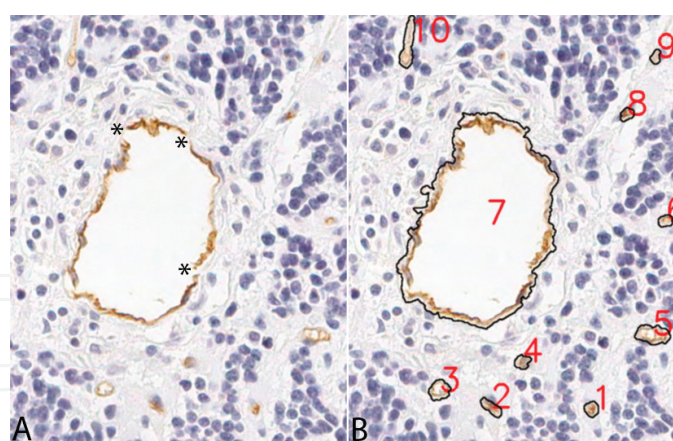
Figure 8. Segmentation process on a neuroblastic tumor sample immunostained with CD31. **A)** Original image. **B)** Image after segmentation. Note that the big blood vessel with an interrupted staining of the endothelial cells surrounding the vascular lumen (asterisk) has been closed, thus providing morphometric measures.

3.3.2.3. Spatial distribution of microenvironmental components

Topological network analysis and the graph theory in combination with Vonoroi tessellations [98] have recently been found to be useful in the diagnosis of muscular dystrophies and

neurogenic atrophies, in the classification of neuromuscular disease or to model the progression of dementia [99–102]. All the generated information is subject to capture relevant information about the organization of different tissue markers.

3.3.2.4. Texture analysis

Another novel approach to cancer research is the texture analysis of different tissue images and machine-learning methods to train automated algorithms which find different patterns in the tissue capable of discriminating between prognostic groups, among other variables, resulting in computer-aided diagnosis tools [103–106].

4. Therapeutic implications of the study of ECM elements

The accumulation of non-fluid elements in the tumor ECM, understood as an increased density of fibrous elements with huge crosslinking, carries the establishment of a solid pressure within the tumor tissue, which, together with other pressure sources, leads to an elevated tumor interstitial pressure [107]. Elevated tumor pressure alters gene expression, cancer cell proliferation, apoptosis and invasiveness, stromal cell function, and ECM synthesis and organization [108–110]. Additionally, it has a negative impact on cancer treatment and is known to reduce the efficacy of cancer therapy through a reduced uptake and heterogeneous distribution of drugs [111, 112]. The direct intratumoral injection of anticancer agents has been evaluated extensively in the past decades, as one approach to counteract such intratumoral pressure [113]. For example, is has been shown that intratumoral injection of immunostimulatory oligonucleotides induces differentiation and reduces immunosuppressive activity of myeloid-derived suppressor cells in mice inoculated with colon cancer cell lines [114]. Regarding ECM fibers, therapies that attack some of the major physical changes themselves, such as inhibiting matrix crosslinking, could be developed to revert pressure within the tumor tissue [115]. Most of the therapeutic strategies under study are based on altering the fibroblastic pathways of collagen synthesis and inhibiting fibroblast growth factor [116–118]. Other strategies focusing on the destruction of existing fibrosis are being developed. In this sense, collagenase has been shown to reduce tumor interstitial pressure by cleaving collagen and consequently destroying the collagen crosslinked networks in human osteosarcoma xenografts [119]. Moreover, this enzyme could indirectly affect tumor ECM by degrading the reticulin fibers associated with blood vessels. Another therapeutic approach not affecting the amount of fibers but the morphology consists in impeding an increased crosslinking. The reduction of lysyl-oxidase-like-2, catalyzing the production of a crosslinked collagenous matrix, by the monoclonal antibody AB0023, was efficacious in reducing disease in different models of cancer and fibrosis [115]. Incorporating biomechanical forces into our current picture of the tumor microenvironment, through the study of the interaction and the status of different ECM elements, fundamentally changes the context in which we study the basic cell and molecular biology of cancer. If there is one core message from the last two decades of research into the tumor ECM, it is that context matters [120].

Solid stresses affect tumor pathophysiology directly by compressing cancer and stromal cells but also indirectly by deforming blood and lymphatic vessels as described in pancreatic cancer, where compressed vessels are observable at the histological level [111]. The compression of tumor vasculature also leads to a reduction in tumor blood flow and subsequently reduces the anticancer agent transport to tumor cells [121]. Therapeutic chemicals are normally transported through the interstitial space by convection, a transport process that is dependent on pressure gradients, but increased tumor vessel permeability creates a less steep gradient along the vessels. This leads to a reduction in convective transport across the vessels in tumor bulk [122]. Additionally, an increase in vessels permeability enables the extravasation of stem and immune cells, among others, and the entrance of malignant cells into the bloodstream to promote metastasis [123]. Moreover, abnormal and tortuous tumor vasculature causes blood stasis, which leads to the reduction of oxygen and blood flow in tumors causing hypoxia and subsequently ischemia and necrosis [121]. This effect increases anabolic metabolism which produce an acid ECM that degrades or deactivates some therapeutic drugs and renders them ineffective [124]. Hypoxia also can cause resistance to radiotherapy and can help tumor cells to escape immunosurveillance [45]. Because of its importance to the tumor, tumor vasculature represents an "Achilles' heel" that can be used for cancer therapy [125]. Indeed, multiple antiangiogenic therapeutic strategies have been developed in the last decades for many different malignancies [57]. Several direct angiogenic inhibitors (angiostatin, endostatin, and thrombospondin) targeting endothelial cells and indirect anti-antiangiogenic agents blocking the production or activity of pro-angiogenic molecules, such as vascular endothelial growth factor (VEGF), have been developed [126]. In this case, again intratumoral injections of adenoviral vectors encoding tumor-targeted immunoconjugates induce a cytotoxic immune response against the neovasculature endothelial cells and tumor cells in mice xenografted with human melanoma cell lines [127]. Recent studies have focused on the value of normalizing tumor vasculature to improve responses to conventional anticancer therapies rather than destroying tumor vessels to starve primary tumors from oxygen and induce tumor shrinkage [128]. Vessel normalization results in reduced vessel diameter, increased pericyte coverage, and normalized basement membrane, accompanied by normalization of its function. This normalized tumor vasculature becomes less permeable and tortuous and leads to reduced fluid and protein extravasation into the interstitium, resulting in the decrease tumor interstitial pressure [129, 130]. For example, various preclinical studies have shown that the high levels of VEGF observed in tumors induce vessel abnormalities [131, 132]. Therefore, targeting VEGF using anti-VEGF antibodies and inhibitors such as bevacizumab has been shown to reduce tumor interstitial pressure [133, 134]. Another protein playing an important role in tumor angiogenesis is PDGF. Imatinib, a PDGFR-inhibitor has been shown to reduce tumor interstitial pressure and enhance therapeutic efficacy [135]. Other drugs such as hydralazine and cachectin are vasodilators that cause a decrease in vascular resistance followed by an increase in tumor blood flow, which can potentially improve intratumoral transport of macromolecules and that have been shown to reduce intratumoral pressure [136, 137]. In addition to these therapeutic agents, some physical approaches have been tested to decrease tumor ECM pressure that can be summarized as follows: irradiation reduces the vascular wall permeability to fluid and leads to a reduction of intratumoral pressure [138]; induced hyperthermia or

hypothermia have shown similar results regarding the reduction of intratumoral pressure as for irradiation [139]; ultrasounds due to mechanical (cavitation) and thermal pressure cause damage to tumor cells and ECM, which increase the interstitial hydraulic conductivity, reduces matrix tension and enhances tumor blood flow [140]; hyperbaric oxygen increases oxygen tension and delivery to tissues [141]; finally, photodynamic therapy impaired microcirculation in tumors [142]. All these strategies are possible by the knowledge of the physiopathology of vascularity in tumors ECM. Most of them are in the experimental phases and others are already in clinical trials.

In the specific case of neuroblastic tumors, many relevant processes, such as stem cell differentiation, neuronal maturation, neurite extension, MYCN expression and the malignant potential and phenotype of tumor cells have all been shown to be influenced by ECM stiffness [1]. In this respect, our group performed a preliminary study where some differences regarding ECM elements could be described between favorable and unfavorable neuroblastic tumors [85]. This study was extended to a cohort of more than 500 samples where a stiffer, crosslinked and less porous ECM was mainly found in unfavorable tumors [143, 144]. Additionally, unfavorable tumors presented a highly vascularized ECM with mostly sinusoid vessels with abnormal morphologies [145]. Some ECM elements morphometric features helped the description of an ultra-high risk subgroup which could beneficiate of novel therapies [146].

Cancer cells often express a variety of abnormal proteins that can serve as targets for an immune response. Although spontaneous immune responses to these antigens can occur, these reactions are rarely sufficient to cause tumor regression; however, the local administration of immune-activating agents can induce tumor-associated inflammation and protective immunity. By binding to their targets, antibodies exercise their functions through several effector mechanisms, including steric inhibition and neutralization, complement activation, and activation of cell-mediated cytotoxicity. Each of these mechanisms may play a role in the antitumor activity of monoclonal antibodies; however, at present the relative importance of these mechanisms is not completely clear. In general, immune adjuvant–based therapies have only proven effective against early stage tumors; yet in this context they can be remarkably effective with minimal risk of serious adverse reactions [147]. Advances in immunotherapy have changed the management of several malignancies, being monoclonal antibodies the most specific targeted therapies currently in use [148]. Therefore, understanding how tumor cells develop immune escape mechanisms and create microenvironments that improve their survival and dissemination and to reach assay normalization seems crucial to achieving optimal treatment [69, 149, 150]. Most notable has been the ability of the anti-CTLA4 antibody, ipilimumab, to achieve a significant increase in survival for patients with metastatic melanoma, for which conventional therapies have failed. In the context of advances in the understanding of how tolerance, immunity and immunosuppression regulate antitumor immune responses together with the advent of targeted therapies, suggesting that active immunotherapy represents a path to obtain a durable and long-lasting response in cancer patients [151]. Five monoclonal antibodies are clinically approved for the treatment of hematologic tumors such as chronic lymphocytic leukemia (alemtuzumab), acute myelogenous leukemia (gemtuzumab), and non-Hodgkin's lymphoma (rituximab, ibritumomab tiuxetan, and tositumomab)

[147]. Cetuximab and panitumumab increase progression-free survival in patients with metastatic colorectal cancer who have previously failed standard chemotherapy and are associated with 10–20% and 10% response rates, respectively [152, 153]. Trastuzumab was the second monoclonal antibody approved for cancer therapy and is used, either alone or in combination with paclitaxel, for the treatment of invasive, HER2/*neu*-positive breast cancer, which represents approximately 20–30% of invasive breast cancers with a response rate of 50% when used in combination with chemotherapy [154]. Bevacizumab is the only monoclonal antibody with anticancer activity that does not directly target malignant cells. Instead, bevacizumab binds VEGF, a critical mediator of tumor angiogenesis. Inhibiting angiogenesis slows the delivery of nutrients and oxygen to tumors, inhibiting growth without severely compromising normal tissue function [155, 156].

5. Conclusions

In cancer biology, tumors are described as complex tissues comprised of heterogeneous neoplastic cells interwoven with tumor associated stroma. The characterization of the ECM elements associated with the tumoral and stromal cells presents opportunities for targeted therapeutic intervention. However, the heterogeneity of tumoral elements dictates that, in order to achieve successful clinical treatment, it is necessary to employ a combination of targeted therapies.

Novel and accurate image analysis algorithms must be developed and used to further investigate about tumor ECM composition and conformation and its relationship with different malignancies prognosis. Digital pathology approaches based on automated image analysis are necessary to obtain standardization, reproducibility, and eliminate observers' biases.

The definition of favorable and unfavorable ECM characteristics, together with the understanding of the fact that biomechanical forces affect cell-cell and cell-matrix crosstalk and alter tumor cells fate, suggests the possibility of developing new therapies that can target the behaviors that arise from these complex interactions and from the heterogeneity of tumor tissues.

Acknowledgements

Author details

Irene Tadeo[1*], Tomás Álvaro[2], Samuel Navarro[1] and Rosa Noguera[1]

*Address all correspondence to: irenetadeo@hotmail.com

1 Pathology Department, Medical School, University of Valencia-INCLIVA, Avda. Blasco Ibañez 15, Valencia, Spain

2 Department of Pathology, Hospital de Tortosa, Verge de la Cinta, IISPV, URV, Tortosa, Spain

References

[1] Lam WA, Cao L, Umesh V, Keung AJ, Sen S, Kumar S. Extracellular matrix rigidity modulates neuroblastoma cell differentiation and N-myc expression. Mol Cancer. 2010;9:35.

[2] Noguera R, Nieto OA, Tadeo I, Farinas F, Alvaro T. Extracellular matrix, biotensegrity and tumor microenvironment. An update and overview. Histology and histopathology. 2012;27(6):693–705.

[3] Kim SH, Turnbull J, Guimond S. Extracellular matrix and cell signalling: the dynamic cooperation of integrin, proteoglycan and growth factor receptor. J Endocrinol. 2011;209(2):139–51.

[4] Hu M, Polyak K. Microenvironmental regulation of cancer development. Curr Opin Genet Dev. 2008;18(1):27–34.

[5] Huang S, Ingber DE. A non-genetic basis for cancer progression and metastasis: self-organizing attractors in cell regulatory networks. Breast Dis. 2006;26:27–54.

[6] Tadeo I, Berbegall AP, Escudero LM, Alvaro T, Noguera R. Biotensegrity of the extracellular matrix: physiology, dynamic mechanical balance, and implications in oncology and mechanotherapy. Front Oncol. 2014;4:39.

[7] Tlsty TD, Coussens LM. Tumor stroma and regulation of cancer development. Annu Rev Pathol. 2006;1:119–50.

[8] Stasinopoulos I, Penet MF, Chen Z, Kakkad S, Glunde K, Bhujwalla ZM. Exploiting the tumor microenvironment for theranostic imaging. NMR Biomed. 2011;24(6):636–47.

[9] Aguilar-Cuenca R, Juanes-Garcia A, Vicente-Manzanares M. Myosin II in mechano-transduction: master and commander of cell migration, morphogenesis, and cancer. Cell Mol Life Sci. 2013.

[10] DuFort CC, Paszek MJ, Weaver VM. Balancing forces: architectural control of mechanotransduction. Nat Rev Mol Cell Biol. 2010;12(5):308–19.

[11] Chandler EM, Seo BR, Califano JP, Andresen Eguiluz RC, Lee JS, Yoon CJ, et al. Implanted adipose progenitor cells as physicochemical regulators of breast cancer. Proc Natl Acad Sci U S A. 2012;109(25):9786–91.

[12] Kalluri R, Zeisberg M. Fibroblasts in cancer. Nat Rev Cancer. 2006;6(5):392–401.

[13] Otranto M, Sarrazy V, Bonte F, Hinz B, Gabbiani G, Desmouliere A. The role of the myofibroblast in tumor stroma remodeling. Cell Adh Migr. 2012;6(3):203–19.

[14] Delnero P, Song YH, Fischbach C. Microengineered tumor models: insights & opportunities from a physical sciences-oncology perspective. Biomed Microdevices. 2013.

[15] Netti PA, Berk DA, Swartz MA, Grodzinsky AJ, Jain RK. Role of extracellular matrix assembly in interstitial transport in solid tumors. Cancer Res. 2000;60(9):2497–503.

[16] Chandler EM, Saunders MP, Yoon CJ, Gourdon D, Fischbach C. Adipose progenitor cells increase fibronectin matrix strain and unfolding in breast tumors. Phys Biol. 2011;8(1):015008.

[17] Hinz B. Tissue stiffness, latent TGF-beta1 activation, and mechanical signal transduction: implications for the pathogenesis and treatment of fibrosis. Curr Rheumatol Rep. 2009;11(2):120-6.

[18] Levental KR, Yu H, Kass L, Lakins JN, Egeblad M, Erler JT, et al. Matrix crosslinking forces tumor progression by enhancing integrin signaling. Cell. 2009;139(5):891–906.

[19] Mammoto A, Connor KM, Mammoto T, Yung CW, Huh D, Aderman CM, et al. A mechanosensitive transcriptional mechanism that controls angiogenesis. Nature. 2009;457(7233):1103-8.

[20] Willis AL, Sabeh F, Li XY, Weiss SJ. Extracellular matrix determinants and the regulation of cancer cell invasion stratagems. J Microsc. 2013;251(3):250–60.

[21] Pathak A, Kumar S. From molecular signal activation to locomotion: an integrated, multiscale analysis of cell motility on defined matrices. PloS one. 2011;6(3):e18423.

[22] Zaman MH, Trapani LM, Sieminski AL, Mackellar D, Gong H, Kamm RD, et al. Migration of tumor cells in 3D matrices is governed by matrix stiffness along with cell-matrix adhesion and proteolysis. Proc Natl Acad Sci U S A. 2006;103(29):10889–94.

[23] Carey SP, Kraning-Rush CM, Williams RM, Reinhart-King CA. Biophysical control of invasive tumor cell behavior by extracellular matrix microarchitecture. Biomaterials. 2012;33(16):4157–65.

[24] Delnero P, Song YH, Fischbach C. Microengineered tumor models: insights & opportunities from a physical sciences-oncology perspective. Biomed Microdevices.

[25] Pathak A, Kumar S. Independent regulation of tumor cell migration by matrix stiffness and confinement. Proc Natl Acad Sci U S A. 2012;109(26):10334-9.

[26] Cross SE, Jin YS, Rao J, Gimzewski JK. Nanomechanical analysis of cells from cancer patients. Nat Nanotechnol. 2007;2(12):780-3.

[27] Lekka M, Laidler P, Gil D, Lekki J, Stachura Z, Hrynkiewicz AZ. Elasticity of normal and cancerous human bladder cells studied by scanning force microscopy. Eur Biophys J. 1999;28(4):312-6.

[28] Karamanos NK, Tzanakakis GN. Glycosaminoglycans: from "cellular glue" to novel therapeutical agents. Curr Opin Pharmacol. 2012.

[29] Afratis N, Gialeli C, Nikitovic D, Tsegenidis T, Karousou E, Theocharis AD, et al. Glycosaminoglycans: key players in cancer cell biology and treatment#. FEBS J. 2012.

[30] Bai X, Zhou D, Brown JR, Crawford BE, Hennet T, Esko JD. Biosynthesis of the linkage region of glycosaminoglycans: cloning and activity of galactosyltransferase II, the sixth member of the beta 1,3-galactosyltransferase family (beta 3GalT6). J Biol Chem. 2001;276(51):48189–95.

[31] Zhang L. Glycosaminoglycan (GAG) biosynthesis and GAG-binding proteins. Prog Mol Biol Transl Sci. 2010;93:1–17.

[32] Victor XV, Nguyen TK, Ethirajan M, Tran VM, Nguyen KV, Kuberan B. Investigating the elusive mechanism of glycosaminoglycan biosynthesis. J Biol Chem. 2009;284(38): 25842–53.

[33] Theocharis AD, Skandalis SS, Tzanakakis GN, Karamanos NK. Proteoglycans in health and disease: novel roles for proteoglycans in malignancy and their pharmacological targeting. FEBS J. 2010;277(19):3904–23.

[34] Edwards IJ. Proteoglycans in prostate cancer. Nat Rev Urol. 2012;9(4):196–206.

[35] Sironen RK, Tammi M, Tammi R, Auvinen PK, Anttila M, Kosma VM. Hyaluronan in human malignancies. Exp Cell Res. 2011;317(4):383–91.

[36] Weyers A, Yang B, Yoon DS, Park JH, Zhang F, Lee KB, et al. A structural analysis of glycosaminoglycans from lethal and nonlethal breast cancer tissues: toward a novel class of theragnostics for personalized medicine in oncology? OMICS. 2012;16(3):79–89.

[37] Lowery JL, Datta N, Rutledge GC. Effect of fiber diameter, pore size and seeding method on growth of human dermal fibroblasts in electrospun poly(epsilon-caprolactone) fibrous mats. Biomaterials. 2010;31(3):491–504.

[38] Alberts B, Johnson A, Lewis J, Raff M, Roberts K, Walter P. Molecular Biology of the Cell. 5th ed. New York: Garland Science; 2008.

[39] Ushiki T. Collagen fibers, reticular fibers and elastic fibers. A comprehensive under-standing from a morphological viewpoint. Arch Histol Cytol. 2002;65(2):109–26.

[40] Egeblad M, Rasch MG, Weaver VM. Dynamic interplay between the collagen scaffold and tumor evolution. Curr Opin Cell Biol. 2010;22(5):697–706.

[41] Ren YJ, Zhang S, Mi R, Liu Q, Zeng X, Rao M, et al. Enhanced differentiation of human neural crest stem cells towards the Schwann cell lineage by aligned electrospun fiber matrix. Acta Biomater. 2013;9(8):7727–36.

[42] Ng MR, Brugge JS. A stiff blow from the stroma: collagen crosslinking drives tumor progression. Cancer Cell. 2009;16(6):455-7.

[43] Fukuda T, Tsuneyoshi M. Adhesion proteins, cellular morphology and fibrous components around the cell/extracellular-matrix interface in myxoid liposarcomas. J Cancer Res Clin Oncol. 2000;126(6):320-4.

[44] Yu E, Lee I. Reticular network of the human thymus. J Korean Med Sci. 1993;8(6):431-6.

[45] Choi IK, Strauss R, Richter M, Yun CO, Lieber A. Strategies to increase drug penetration in solid tumors. Front Oncol. 2013;3:193.

[46] Sun Y, Nelson PS. Molecular pathways: involving microenvironment damage respons-es in cancer therapy resistance. Clinical cancer research : an official journal of the American Association for Cancer Research. 2012;18(15):4019–25.

[47] Cheon DJ, Tong Y, Sim MS, Dering J, Berel D, Cui X, et al. A collagen-remodeling gene signature regulated by TGFbeta signaling is associated with metastasis and poor survival in serous ovarian cancer. Clinical cancer research : an official journal of the American Association for Cancer Research. 2013.

[48] Provenzano PP, Eliceiri KW, Campbell JM, Inman DR, White JG, Keely PJ. Collagen reorganization at the tumor-stromal interface facilitates local invasion. BMC Med. 2006;4(1):38.

[49] Urban Z, Boyd CD. Elastic-fiber pathologies: primary defects in assembly and secon-dary disorders in transport and delivery. Am J Hum Genet. 2000;67(1):4-7.

[50] Agrawal U, Rai H, Jain AK. Morphological and ultrastructural characteristics of extracellular matrix changes in oral squamous cell carcinoma. Indian J Dent Res. 2011;22(1):16–21.

[51] Toupance S, Brassart B, Rabenoelina F, Ghoneim C, Vallar L, Polette M, et al. Elastin-derived peptides increase invasive capacities of lung cancer cells by post-transcrip-tional regulation of MMP-2 and uPA. Clin Exp Metastasis. 2012;29(5):511–22.

[52] Devy J, Duca L, Cantarelli B, Joseph-Pietras D, Scandolera A, Rusciani A, et al. Elastin-derived peptides enhance melanoma growth in vivo by upregulating the activation of Mcol-A (MMP-1) collagenase. British journal of cancer. 2012;103(10):1562–70.

[53] Chang YS, di Tomaso E, McDonald DM, Jones R, Jain RK, Munn LL. Mosaic blood vessels in tumors: frequency of cancer cells in contact with flowing blood. Proc Natl Acad Sci U S A. 2000;97(26):14608–13.

[54] Hillen F, Griffioen AW. Tumour vascularization: sprouting angiogenesis and beyond. Cancer Metastasis Rev. 2007;26(3-4):489–502.

[55] Styp-Rekowska B, Hlushchuk R, Pries AR, Djonov V. Intussusceptive angiogenesis: pillars against the blood flow. Acta Physiol (Oxf). 2011;202(3):213–23.

[56] Bergers G, Benjamin LE. Tumorigenesis and the angiogenic switch. Nat Rev Cancer. 2003;3(6):401–10.

[57] Carmeliet P, Jain RK. Angiogenesis in cancer and other diseases. Nature. 2000;407(6801):249–57.

[58] Ichihara E, Kiura K, Tanimoto M. Targeting angiogenesis in cancer therapy. Acta Med Okayama. 2011;65(6):353–62.

[59] Weis SM, Cheresh DA. Tumor angiogenesis: molecular pathways and therapeutic targets. Nat Med. 2011;17(11):1359–70.

[60] Canete A, Navarro S, Bermudez J, Pellin A, Castel V, Llombart-Bosch A. Angiogenesis in neuroblastoma: relationship to survival and other prognostic factors in a cohort of neuroblastoma patients. Journal of clinical oncology : official journal of the American Society of Clinical Oncology. 2000;18(1):27–34.

[61] Jakovljevic G, Culic S, Stepan J, Kosuta I, Seiwerth S. Relationship between tumor vascularity and vascular endothelial growth factor as prognostic factors for patients with neuroblastoma. Coll Antropol. 2011;35(4):1071-9.

[62] Meitar D, Crawford SE, Rademaker AW, Cohn SL. Tumor angiogenesis correlates with metastatic disease, N-myc amplification, and poor outcome in human neuroblastoma. Journal of clinical oncology : official journal of the American Society of Clinical Oncology. 1996;14(2):405–14.

[63] Ozer E, Altungoz O, Unlu M, Aygun N, Tumer S, Olgun N. Association of MYCN amplification and 1p deletion in neuroblastomas with high tumor vascularity. Appl Immunohistochem Mol Morphol. 2007;15(2):181-6.

[64] Peddinti R, Zeine R, Luca D, Seshadri R, Chlenski A, Cole K, et al. Prominent micro-vascular proliferation in clinically aggressive neuroblastoma. Clinical cancer research : an official journal of the American Association for Cancer Research. 2007;13(12):3499–506.

[65] Ribatti D, Surico G, Vacca A, De Leonardis F, Lastilla G, Montaldo PG, et al. Angio-genesis extent and expression of matrix metalloproteinase-2 and -9 correlate with progression in human neuroblastoma. Life Sci. 2001;68(10):1161-8.

[66] Galon J, Pages F, Marincola FM, Angell HK, Thurin M, Lugli A, et al. Cancer classifi-cation using the Immunoscore: a worldwide task force. Journal of translational medicine. 2012;10:205.

[67] Martinet L, Garrido I, Filleron T, Le Guellec S, Bellard E, Fournie JJ, et al. Human solid tumors contain high endothelial venules: association with T- and B-lymphocyte infiltration and favorable prognosis in breast cancer. Cancer Res. 2011;71(17):5678–87.

[68] Rahir G, Moser M. Tumor microenvironment and lymphocyte infiltration. Cancer Immunol Immunother. 2012;61(6):751-9.

[69] Fridman WH, Galon J, Pages F, Tartour E, Sautes-Fridman C, Kroemer G. Prognostic and predictive impact of intra- and peritumoral immune infiltrates. Cancer Res. 2011;71(17):5601-5.

[70] Galon J, Fridman WH, Pages F. The adaptive immunologic microenvironment in colorectal cancer: a novel perspective. Cancer Res. 2007;67(5):1883-6.

[71] Wang E, Miller LD, Ohnmacht GA, Mocellin S, Perez-Diez A, Petersen D, et al. Prospective molecular profiling of melanoma metastases suggests classifiers of immune responsiveness. Cancer Res. 2002;62(13):3581-6.

[72] Fridman WH, Pages F, Sautes-Fridman C, Galon J. The immune contexture in human tumours: impact on clinical outcome. Nat Rev Cancer. 2012;12(4):298–306.

[73] Nosho K, Baba Y, Tanaka N, Shima K, Hayashi M, Meyerhardt JA, et al. Tumour-infiltrating T-cell subsets, molecular changes in colorectal cancer, and prognosis: cohort study and literature review. The Journal of pathology. 2010;222(4):350–66.

[74] Ogino S, Nosho K, Irahara N, Meyerhardt JA, Baba Y, Shima K, et al. Lymphocytic reaction to colorectal cancer is associated with longer survival, independent of lymph node count, microsatellite instability, and CpG island methylator phenotype. Clinical cancer research : an official journal of the American Association for Cancer Research. 2009;15(20):6412–20.

[75] Pages F, Kirilovsky A, Mlecnik B, Asslaber M, Tosolini M, Bindea G, et al. In situ cytotoxic and memory T cells predict outcome in patients with early-stage colorectal cancer. Journal of clinical oncology : official journal of the American Society of Clinical Oncology. 2009;27(35):5944–51.

[76] Wang H, Zhang W, Fuller GN. Tissue microarrays: applications in neuropathology research, diagnosis, and education. Brain Pathol. 2002;12(1):95–107.

[77] Henshall S. Tissue microarrays. J Mammary Gland Biol Neoplasia. 2003;8(3):347–58.

[78] Avninder S, Ylaya K, Hewitt SM. Tissue microarray: A simple technology that has revolutionized research in pathology. J Postgrad Med. 2008;54(2):158–62.

[79] Brown LA, Huntsman D. Fluorescent in situ hybridization on tissue microarrays: challenges and solutions. J Mol Histol. 2007;38(2):151-7.

[80] Hassan S, Ferrario C, Mamo A, Basik M. Tissue microarrays: emerging standard for biomarker validation. Curr Opin Biotechnol. 2008;19(1):19–25.

[81] Pham DL, Xu C, Prince JL. Current methods in medical image segmentation. Annu Rev Biomed Eng. 2000;2:315–37.

[82] Peces C, Garcia-Rojo M, Sacristan J, Gallardo AJ, Rodriguez A. Serendipia: Castilla-La Mancha telepathology network. Diagn Pathol. 2008;3 Suppl 1:S5.

[83] Slodkowska J, Garcia-Rojo M. Digital pathology in personalized cancer therapy. Studies in health technology and informatics. 2012;179:143–54.

[84] Rojo MG, Bueno G, Slodkowska J. Review of imaging solutions for integrated quantitative immunohistochemistry in the Pathology daily practice. Folia histochemica et cytobiologica / Polish Academy of Sciences, Polish Histochemical and Cytochemical Society. 2009;47(3):349–54.

[85] Tadeo I, Piqueras M, Montaner D, Villamon E, Berbegall AP, Canete A, et al. Quantitative modeling of clinical, cellular, and extracellular matrix variables suggest prognostic indicators in cancer: a model in neuroblastoma. Pediatric research. 2014;75(2): 302–14.

[86] Thiele J, Kvasnicka HM, Facchetti F, Franco V, van der Walt J, Orazi A. European consensus on grading bone marrow fibrosis and assessment of cellularity. Haematologica. 2005;90(8):1128–32.

[87] Chen LB, Huang HH, Shu X, Xu QH, Chen N, Zhang K, et al. [Pathological study of liver biopsy from 156 patients clinically diagnosed with mild chronic hepatitis B based on current guideline]. Zhonghua Shi Yan He Lin Chuang Bing Du Xue Za Zhi. 2009;23(2):138–40.

[88] Caballero T, Perez-Milena A, Masseroli M, O'Valle F, Salmeron FJ, Del Moral RM, et al. Liver fibrosis assessment with semiquantitative indexes and image analysis quantification in sustained-responder and non-responder interferon-treated patients with chronic hepatitis C. J Hepatol. 2001;34(5):740-7.

[89] Duregon E, Fassina A, Volante M, Nesi G, Santi R, Gatti G, et al. The reticulin algorithm for adrenocortical tumor diagnosis: a multicentric validation study on 245 unpublished cases. Am J Surg Pathol. 2013;37(9):1433–40.

[90] Huss S, Schmitz J, Goltz D, Fischer HP, Buttner R, Weiskirchen R. Development and evaluation of an open source Delphi-based software for morphometric quantification of liver fibrosis. Fibrogenesis Tissue Repair. 2010;3(1):10.

[91] Vertemati M, Moscheni C, Petrella D, Lamperti L, Cossa M, Gambacorta M, et al. Morphometric analysis of hepatocellular nodular lesions in HCV cirrhosis. Pathol Res Pract. 2012;208(4):240-4.

[92] Vertemati M, Vizzotto L, Moscheni C, Dhillon A, Quaglia A. A morphometric model to minimize subjectivity in the histological assessment of hepatocellular carcinoma and its precursors in cirrhosis. Microsc Res Tech. 2008;71(8):606–13.

[93] Teman CJ, Wilson AR, Perkins SL, Hickman K, Prchal JT, Salama ME. Quantification of fibrosis and osteosclerosis in myeloproliferative neoplasms: a computer-assisted image study. Leuk Res. 2010;34(7):871-6.

[94] Korkolopoulou P, Patsouris E, Kavantzas N, Konstantinidou AE, Christodoulou P, Thomas-Tsagli E, et al. Prognostic implications of microvessel morphometry in diffuse astrocytic neoplasms. Neuropathol Appl Neurobiol. 2002;28(1):57–66.

[95] Laitakari J, Nayha V, Stenback F. Size, shape, structure, and direction of angiogenesis in laryngeal tumour development. J Clin Pathol. 2004;57(4):394–401.

[96] Fernández-Carrobles MM, Tadeo I, Bueno G, Noguera R, Navarro S, Déniz O, et al. TMA vessel segmentation based on color and morphological features. Application to angiogenesis research. Journal of Biomedicine and Biotechnology. 2013:Aceptado para publicación.

[97] Fernández-Carrobles MM, Tadeo I, Noguera R, Navarro S, García-Rojo M, Déniz O, et al., editors. A morphometric tool applied to angiogenesis research based on vessel segmentation. Diagnostic Pathology; 2013.

[98] Voronoi GF. Nouvelles applications des paramètres continus à la théorie de formes quadratiques. Journal für die reine und angewandte Mathematik 1908;134:198–287.

[99] Barabasi AL, Oltvai ZN. Network biology: understanding the cell's functional organization. Nat Rev Genet. 2004;5(2):101–13.

[100] Raj A, Kuceyeski A, Weiner M. A network diffusion model of disease progression in dementia. Neuron. 2012;73(6):1204–15.

[101] Saez A, Acha B, Montero-Sanchez A, Rivas E, Escudero LM, Serrano C. Neuromuscular disease classification system. J Biomed Opt. 2013;18(6):066017.

[102] Saez A, Rivas E, Montero-Sanchez A, Paradas C, Acha B, Pascual A, et al. Quantifiable diagnosis of muscular dystrophies and neurogenic atrophies through network analysis. BMC Med. 2013;11:77.

[103] Ganeshan B, Miles KA. Quantifying tumour heterogeneity with CT. Cancer Imaging. 2013;13:140-9.

[104] Kalinli A, Sarikoc F, Akgun H, Ozturk F. Performance comparison of machine learning methods for prognosis of hormone receptor status in breast cancer tissue samples. Comput Methods Programs Biomed. 2013;110(3):298–307.

[105] Kowal M, Filipczuk P, Obuchowicz A, Korbicz J, Monczak R. Computer-aided diagnosis of breast cancer based on fine needle biopsy microscopic images. Computers in biology and medicine. 2013;43(10):1563–72.

[106] Ninos K, Kostopoulos S, Sidiropoulos K, Kalatzis I, Glotsos D, Athanasiadis E, et al. Computer-based image analysis system designed to differentiate between low-grade and high-grade laryngeal cancer cases. Anal Quant Cytol Histol. 2013;35(5):261–72.

[107] Stylianopoulos T, Martin JD, Snuderl M, Mpekris F, Jain SR, Jain RK. Coevolution of solid stress and interstitial fluid pressure in tumors during progression: implications for vascular collapse. Cancer Res. 2013;73(13):3833–41.

[108] Demou ZN. Gene expression profiles in 3D tumor analogs indicate compressive strain differentially enhances metastatic potential. Annals of biomedical engineering. 2010;38(11):3509–20.

[109] Paszek MJ, Weaver VM. The tension mounts: mechanics meets morphogenesis and malignancy. J Mammary Gland Biol Neoplasia. 2004;9(4):325–42.

[110] Tse JM, Cheng G, Tyrrell JA, Wilcox-Adelman SA, Boucher Y, Jain RK, et al. Mechanical compression drives cancer cells toward invasive phenotype. Proc Natl Acad Sci U S A. 2012;109(3):911-6.

[111] Jain RK, Baxter LT. Mechanisms of heterogeneous distribution of monoclonal antibodies and other macromolecules in tumors: significance of elevated interstitial pressure. Cancer Res. 1988;48(24 Pt 1):7022–32.

[112] Salmon H, Franciszkiewicz K, Damotte D, Dieu-Nosjean MC, Validire P, Trautmann A, et al. Matrix architecture defines the preferential localization and migration of T cells into the stroma of human lung tumors. J Clin Invest. 2012;122(3):899–910.

[113] Lammers T, Peschke P, Kuhnlein R, Subr V, Ulbrich K, Huber P, et al. Effect of intratumoral injection on the biodistribution and the therapeutic potential of HPMA copolymer-based drug delivery systems. Neoplasia. 2006;8(10):788–95.

[114] Shirota Y, Shirota H, Klinman DM. Intratumoral injection of CpG oligonucleotides induces the differentiation and reduces the immunosuppressive activity of myeloid-derived suppressor cells. Journal of immunology. 2012;188(4):1592-9.

[115] Barry-Hamilton V, Spangler R, Marshall D, McCauley S, Rodriguez HM, Oyasu M, et al. Allosteric inhibition of lysyl oxidase-like-2 impedes the development of a pathologic microenvironment. Nat Med. 2010;16(9):1009–17.

[116] Kendall RT, Feghali-Bostwick CA. Fibroblasts in fibrosis: novel roles and mediators. Front Pharmacol. 2014;5:123.

[117] Loeffler M, Kruger JA, Niethammer AG, Reisfeld RA. Targeting tumor-associated fibroblasts improves cancer chemotherapy by increasing intratumoral drug uptake. J Clin Invest. 2006;116(7):1955–62.

[118] Ostapoff KT, Kutluk Cenik B, Wang M, Ye R, Xu X, Nugent D, et al. Neutralizing murine TGFbetaR2 promotes a differentiated tumor cell phenotype and inhibits pancreatic cancer metastasis. Cancer Res. 2014.

[119] Eikenes L, Bruland OS, Brekken C, Davies Cde L. Collagenase increases the transcapillary pressure gradient and improves the uptake and distribution of monoclonal antibodies in human osteosarcoma xenografts. Cancer Res. 2004;64(14):4768–73.

[120] Shieh AC. Biomechanical forces shape the tumor microenvironment. Annals of biomedical engineering. 2011;39(5):1379–89.

[121] Padera TP, Stoll BR, Tooredman JB, Capen D, di Tomaso E, Jain RK. Pathology: cancer cells compress intratumour vessels. Nature. 2004;427(6976):695.

[122] Ariffin AB, Forde PF, Jahangeer S, Soden DM, Hinchion J. Releasing pressure in tumors: what do we know so far and where do we go from here? A review. Cancer Res. 2014;74(10):2655–62.

[123] Reymond N, d'Agua BB, Ridley AJ. Crossing the endothelial barrier during metastasis. Nat Rev Cancer. 2013;13(12):858–70.

[124] Vaupel P, Kallinowski F, Okunieff P. Blood flow, oxygen and nutrient supply, and metabolic microenvironment of human tumors: a review. Cancer Res. 1989;49(23): 6449–65.

[125] Johannessen TC, Wagner M, Straume O, Bjerkvig R, Eikesdal HP. Tumor vasculature: the Achilles' heel of cancer? Expert opinion on therapeutic targets. 2013;17(1):7–20.

[126] Rossler J, Taylor M, Geoerger B, Farace F, Lagodny J, Peschka-Suss R, et al. Angiogenesis as a target in neuroblastoma. Eur J Cancer. 2008;44(12):1645–56.

[127] Hu Z, Garen A. Intratumoral injection of adenoviral vectors encoding tumor-targeted immunoconjugates for cancer immunotherapy. Proc Natl Acad Sci U S A. 2000;97(16): 9221-5.

[128] Carmeliet P, Jain RK. Principles and mechanisms of vessel normalization for cancer and other angiogenic diseases. Nat Rev Drug Discov. 2011;10(6):417–27.

[129] Goel S, Wong AH, Jain RK. Vascular normalization as a therapeutic strategy for malignant and nonmalignant disease. Cold Spring Harb Perspect Med. 2012;2(3):a006486.

[130] Jain RK, Tong RT, Munn LL. Effect of vascular normalization by antiangiogenic therapy on interstitial hypertension, peritumor edema, and lymphatic metastasis: insights from a mathematical model. Cancer Res. 2007;67(6):2729–35.

[131] Baffert F, Le T, Sennino B, Thurston G, Kuo CJ, Hu-Lowe D, et al. Cellular changes in normal blood capillaries undergoing regression after inhibition of VEGF signaling. Am J Physiol Heart Circ Physiol. 2006;290(2):H547–59.

[132] Jain RK. Normalization of tumor vasculature: an emerging concept in antiangiogenic therapy. Science. 2005;307(5706):58–62.

[133] Salnikov AV, Heldin NE, Stuhr LB, Wiig H, Gerber H, Reed RK, et al. Inhibition of carcinoma cell-derived VEGF reduces inflammatory characteristics in xenograft carcinoma. Int J Cancer. 2006;119(12):2795–802.

[134] Tong RT, Boucher Y, Kozin SV, Winkler F, Hicklin DJ, Jain RK. Vascular normalization by vascular endothelial growth factor receptor 2 blockade induces a pressure gradient across the vasculature and improves drug penetration in tumors. Cancer Res. 2004;64(11):3731-6.

[135] Fan Y, Du W, He B, Fu F, Yuan L, Wu H, et al. The reduction of tumor interstitial fluid pressure by liposomal imatinib and its effect on combination therapy with liposomal doxorubicin. Biomaterials. 2013;34(9):2277–88.

[136] Jarm T, Podobnik B, Sersa G, Miklavcic D. Effect of hydralazine on blood flow, oxygenation, and interstitial fluid pressure in subcutaneous tumors. Adv Exp Med Biol. 2003;510:25-9.

[137] Kristensen CA, Nozue M, Boucher Y, Jain RK. Reduction of interstitial fluid pressure after TNF-alpha treatment of three human melanoma xenografts. British journal of cancer. 1996;74(4):533-6.

[138] Multhoff G, Vaupel P. Radiation-induced changes in microcirculation and interstitial fluid pressure affecting the delivery of macromolecules and nanotherapeutics to tumors. Front Oncol. 2012;2:165.

[139] Sen A, Capitano ML, Spernyak JA, Schueckler JT, Thomas S, Singh AK, et al. Mild elevation of body temperature reduces tumor interstitial fluid pressure and hypoxia and enhances efficacy of radiotherapy in murine tumor models. Cancer Res. 2011;71(11):3872–80.

[140] Watson KD, Lai CY, Qin S, Kruse DE, Lin YC, Seo JW, et al. Ultrasound increases nanoparticle delivery by reducing intratumoral pressure and increasing transport in epithelial and epithelial-mesenchymal transition tumors. Cancer Res. 2012;72(6):1485–93.

[141] Stuhr LE, Raa A, Oyan AM, Kalland KH, Sakariassen PO, Petersen K, et al. Hyperoxia retards growth and induces apoptosis, changes in vascular density and gene expression in transplanted gliomas in nude rats. J Neurooncol. 2007;85(2):191–202.

[142] Kleemann B, Loos B, Scriba TJ, Lang D, Davids LM. St John's Wort (Hypericum perforatum L.) Photomedicine: Hypericin-Photodynamic Therapy Induces Metastatic Melanoma Cell Death. PloS one. 2014;9(7):e103762.

[143] Tadeo I. Study of the architectural scaffolding and the vascular system of neuroblastic tumors. Valencia, Spain: University of Valencia; 2015.

[144] Tadeo I, Berbegall AP, Navarro S, Castel V, Noguera R. Extracellular matrix histological patterns are associated to malignancy in Neuroblastic tumors. Manuscript in preparation. 2016.

[145] Tadeo I, Bueno G, Berbegall AP, Fernández-Carrobles MM, Castel V, Garcia-Rojo M, et al. Vascular patterns provide therapeutic targets in aggressive neuroblastic tumors. Under consideration in Oncotarget. 2016.

[146] Tadeo I, Berbegall AP, Castel V, García-Miguel P, Callaghan R, Påhlman S, et al. Extracellular Matrix Composition defines an Ultra-High Risk Group of Neuroblastoma within the High Risk Patient Cohort. Under consideration in British Journal of Cancer. 2016.

[147] Dougan M, Dranoff G. Immune therapy for cancer. Annual review of immunology. 2009;27:83–117.

[148] Neves H, Kwok HF. Recent advances in the field of anti-cancer immunotherapy. BBA clinical. 2015;3:280-8.

[149] Seeger RC. Immunology and immunotherapy of neuroblastoma. Semin Cancer Biol. 2011;21(4):229–37.

[150] Kerkar SP, Restifo NP. Cellular constituents of immune escape within the tumor microenvironment. Cancer Res. 2012;72(13):3125–30.

[151] Mellman I, Coukos G, Dranoff G. Cancer immunotherapy comes of age. Nature. 2011;480(7378):480-9.

[152] Meyerhardt JA, Mayer RJ. Systemic therapy for colorectal cancer. N Engl J Med. 2005;352(5):476–87.

[153] Van Cutsem E, Peeters M, Siena S, Humblet Y, Hendlisz A, Neyns B, et al. Open-label phase III trial of panitumumab plus best supportive care compared with best supportive care alone in patients with chemotherapy-refractory metastatic colorectal cancer. Journal of clinical oncology : official journal of the American Society of Clinical Oncology. 2007;25(13):1658–64.

[154] Hudis CA. Trastuzumab--mechanism of action and use in clinical practice. N Engl J Med. 2007;357(1):39–51.

[155] Cohen MH, Gootenberg J, Keegan P, Pazdur R. FDA drug approval summary: bevacizumab (Avastin) plus Carboplatin and Paclitaxel as first-line treatment of advanced/metastatic recurrent nonsquamous non-small cell lung cancer. The oncologist. 2007;12(6):713-8.

[156] Cohen MH, Gootenberg J, Keegan P, Pazdur R. FDA drug approval summary: bevacizumab plus FOLFOX4 as second-line treatment of colorectal cancer. The oncologist. 2007;12(3):356–61.